2013

The ubiquitin receptor S5a/Rpn10 links centrosomal proteasomes with dendrite development in the mammalian brain

Sidharth V. Puram
Harvard University

Albert H. Kim
Washington University School of Medicine in St. Louis

Hye-Yeon Park
Harvard University

Julius Anckar
Harvard University

Azad Bonni
Washington University School of Medicine in St. Louis

Follow this and additional works at: http://digitalcommons.wustl.edu/open_access_pubs

Recommended Citation

Puram, Sidharth V.; Kim, Albert H.; Park, Hye-Yeon; Anckar, Julius; and Bonni, Azad , "The ubiquitin receptor S5a/Rpn10 links centrosomal proteasomes with dendrite development in the mammalian brain." Cell Reports.4,1. 19-30. (2013).
http://digitalcommons.wustl.edu/open_access_pubs/1531

The Ubiquitin Receptor S5a/Rpn10 Links Centrosomal Proteasomes with Dendrite Development in the Mammalian Brain

Sidharth V. Puram,[1,2,7] Albert H. Kim,[3,4,7,*] Hye-Yeon Park,[1,4,5] Julius Anckar,[1] and Azad Bonni[1,2,5,6,*]
[1]Department of Neurobiology, Harvard Medical School, Boston, MA 02115, USA
[2]Program in Biological and Biomedical Sciences, Harvard Medical School, Boston, MA 02115, USA
[3]Department of Neurosurgery, Washington University School of Medicine, St. Louis, MO 63110, USA
[4]Department of Neurosurgery, Brigham and Women's Hospital, Boston, MA 02115, USA
[5]Program in Neuroscience, Harvard Medical School, Boston, MA 02115, USA
[6]Department of Anatomy and Neurobiology, Washington University School of Medicine, St. Louis, MO 63110, USA
[7]These authors contributed equally to this work
*Correspondence: kima@wudosis.wustl.edu (A.H.K.), bonni@wustl.edu (A.B.)
http://dx.doi.org/10.1016/j.celrep.2013.06.006

SUMMARY

Proteasomes drive the selective degradation of protein substrates with covalently linked ubiquitin chains in eukaryotes. Although proteasomes are distributed throughout the cell, specific biological functions of the proteasome in distinct subcellular locales remain largely unknown. We report that proteasomes localized at the centrosome regulate the degradation of local ubiquitin conjugates in mammalian neurons. We find that the proteasomal subunit S5a/Rpn10, a ubiquitin receptor that selects substrates for degradation, is essential for proteasomal activity at centrosomes in neurons and thereby promotes the elaboration of dendrite arbors in the rodent brain in vivo. We also find that the helix-loop-helix protein Id1 disrupts the interaction of S5a/Rpn10 with the proteasomal lid and thereby inhibits centrosomal proteasome activity and dendrite elaboration in neurons. Together, our findings define a function for a specific pool of proteasomes at the neuronal centrosome and identify a biological function for S5a/Rpn10 in the mammalian brain.

INTRODUCTION

The ubiquitin-proteasome system regulates diverse biological processes, including aspects of neuronal development ranging from axon morphogenesis to the formation and refinement of synapses (Mabb and Ehlers, 2010). After ubiquitin conjugation, substrates are targeted to the proteasome for degradation. Although the mechanism of ubiquitin conjugation through the sequential action of E1, E2, and E3 ubiquitin ligases has been intensely studied (Hershko and Ciechanover, 1998), the pathways linking ubiquitin conjugates to the proteasome are just beginning to be characterized.

The proteasome consists of a 20S catalytic core particle, which cleaves amino acid chains and a 19S regulatory particle (RP) (Besche et al., 2009). The RP protein S5a/Rpn10 is an essential member of the proteasomal lid, acting as a ubiquitin receptor that ushers ubiquitinated proteins to the proteasome (Deveraux et al., 1994; Verma et al., 2004). In yeast, S5a/Rpn10 is required for the degradation of ubiquitin fusion degradation (UFD) pathway substrates (van Nocker et al., 1996), but the biological functions of S5a/Rpn10 in the mammalian brain remain to be defined.

As proteasomes are distributed throughout the cell, a fundamental question is whether the spatial organization of proteasomes dictates specific biological functions. However, with few exceptions (Bingol et al., 2010; Djakovic et al., 2009; O'Connell and Harper, 2007), the roles of proteasomes in subcellular locales remain unknown. Recent studies suggest ubiquitin signaling at the centrosome plays a role in neuronal differentiation (Kim et al., 2009), raising the question of whether proteasomes operate at the centrosome to regulate neuronal morphogenesis in the mammalian brain.

In this study, we report that proteasomes operate at the centrosome to regulate the degradation of local ubiquitin conjugates in mammalian neurons and thereby orchestrate dendrite elaboration. We also uncover a function for the ubiquitin receptor subunit S5a/Rpn10 in the control of proteasome activity at the centrosome in neurons and in the elaboration of dendrite arbors in the rodent brain in vivo. Finally, we find that centrosomally localized helix-loop-helix protein Id1 inhibits S5a/Rpn10-dependent proteasome function at the centrosome in neurons. These findings define a function for a specific pool of proteasomes at the neuronal centrosome and uncover a biological function for S5a/Rpn10 in the brain.
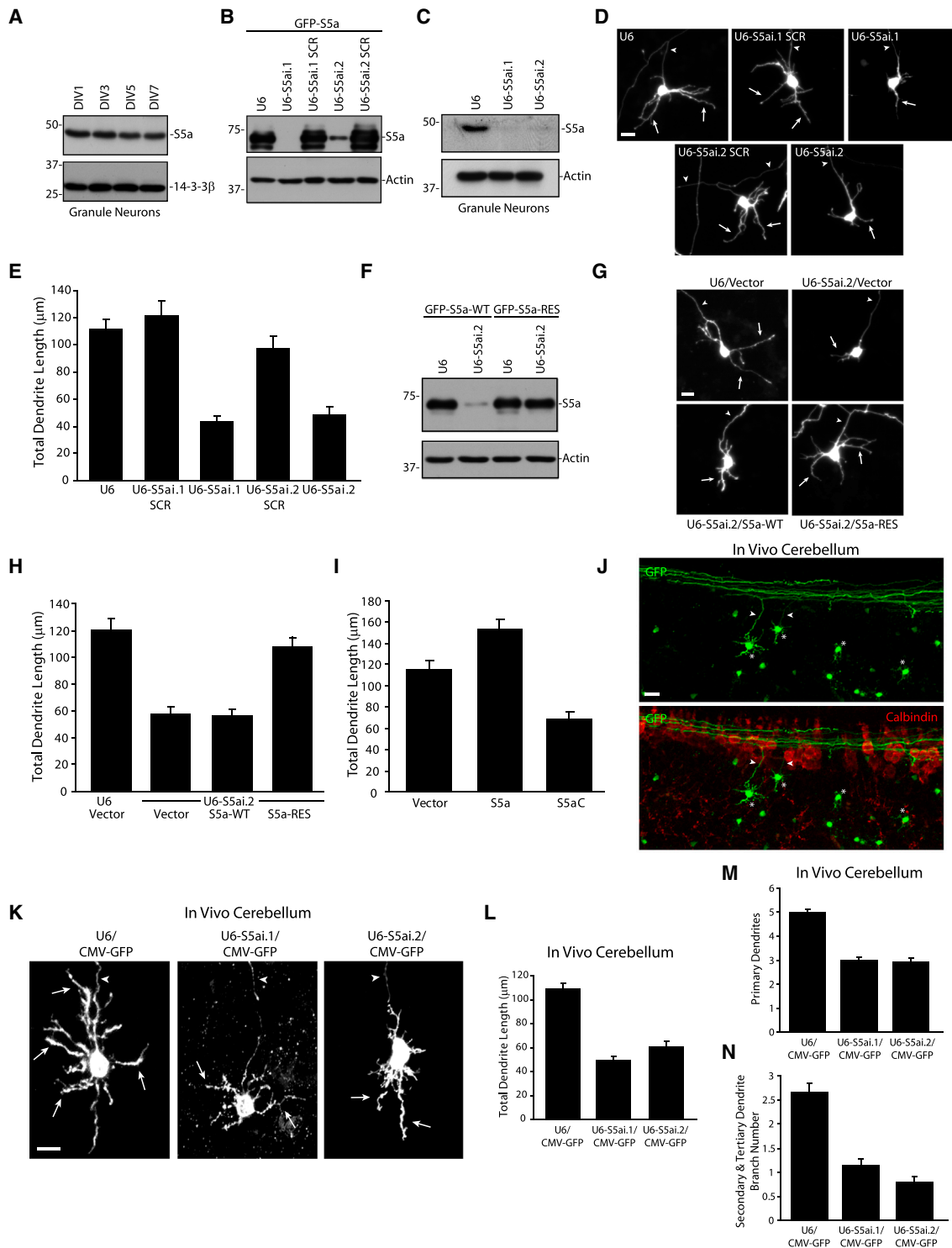
Figure 1. S5a/Rpn10 Is Required for Dendrite Growth and Elaboration in Primary Neurons and in the Rodent Brain In Vivo

(A) Lysates of granule neurons were immunoblotted with indicated antibodies. DIV, days in vitro.

(B) Lysates of 293T cells transfected with a plasmid encoding GFP-S5a together with S5a/Rpn10 RNAi, scrambled S5a/Rpn10 RNAi, or control U6 plasmid were immunoblotted with indicated antibodies.

(C) Lysates of granule neurons electroporated with S5a/Rpn10 RNAi or control U6 plasmid were immunoblotted with indicated antibodies.

(D) Granule neurons transfected with S5a/Rpn10 RNAi plasmids (U6-S5ai), scrambled S5a/Rpn10 RNAi plasmids (U6-S5ai SCR), or control U6 plasmid together with a plasmid encoding GFP were subjected to GFP immunocytochemistry 4 days later. Representative neurons are shown. In all images of neuronal

(legend continued on next page)

RESULTS

S5a/Rpn10 Drives Dendrite Growth and Elaboration in Primary Neurons and in the Rodent Brain In Vivo

We characterized the function of the key proteasomal lid-associated protein S5a/Rpn10 in the mammalian brain, utilizing granule neurons of the developing rat cerebellar cortex. Granule neurons follow a carefully orchestrated program of axon and dendrite morphogenesis that is a prerequisite for the establishment of neuronal connectivity (Hatten and Heintz, 1995). Using an antibody that specifically recognizes S5a/Rpn10, we confirmed S5a/Rpn10 is expressed in primary neurons (Figure 1A).

To determine the function of S5a/Rpn10 in neurons, we used RNA interference (RNAi) to knock down S5a/Rpn10. Expression of two short hairpin RNAs (shRNAs) targeting distinct regions of S5a/Rpn10 but not control scrambled shRNAs reduced the expression of exogenous S5a/Rpn10 in cells (Figure 1B). Expression of S5a/Rpn10 shRNAs also induced the knockdown of endogenous S5a/Rpn10 in neurons (Figure 1C). In assays of neuronal morphology, knockdown of S5a/Rpn10 inhibited dendrite growth, leading to shorter primary dendrites with reduced secondary and tertiary branching (Figure 1D). Quantitation revealed up to a 3-fold reduction in total dendrite length in neurons upon S5a/Rpn10 knockdown (Figure 1E). S5a/Rpn10 RNAi had little or no effect on axon length or neuronal survival (data not shown). These results suggest knockdown of S5a/Rpn10 specifically inhibits the growth and elaboration of dendrites in granule neurons.

To confirm that the S5a/Rpn10 RNAi-induced phenotype is the result of specific knockdown of S5a/Rpn10, we performed a rescue experiment using an expression plasmid encoding S5a/Rpn10 resistant to RNAi (S5a-RES) (Figure 1F). Expression of S5a-RES but not S5a/Rpn10 encoded by wild-type complementary DNA (cDNA) (S5a-WT) restored the characteristic appearance of dendrite arbors and increased dendrite length and branching in the context of S5a/Rpn10 RNAi to that of control transfected neurons (Figures 1G and 1H). These data suggest the S5a/Rpn10 RNAi-induced dendrite phenotype is due to specific knockdown rather than off-target effects of RNAi. In other experiments, expression of S5a/Rpn10 increased dendrite length in granule neurons (Figure 1I), suggesting S5a/Rpn10 exerts a gain-of-function effect on dendrite growth. Expression of a dominant negative form of S5a/Rpn10 (S5aC) that lacks the N-terminal von Willebrand factor A domain required for binding to proteins of the proteasomal lid reduced dendrite length (Figure 1I; Fu et al., 2001). Thus, based on rigorously controlled RNAi, gain-of-function, and dominant interfering approaches, we conclude that S5a/Rpn10 drives the elaboration of dendrite arbors in granule neurons.

We next investigated the role of S5a/Rpn10 in dendrite morphogenesis in the intact developing rat cerebellar cortex. We transfected postnatal day 3 (P3) rat pups with two distinct S5a/Rpn10 RNAi plasmids that also encode GFP (U6-S5ai/CMV-GFP) or the corresponding control RNAi plasmid (U6/CMV-GFP). Transfected rat pups were returned to their mothers and sacrificed 5 days later. Isolated cerebella from P8 pups were subjected to immunohistochemistry using GFP and Calbindin antibodies. GFP-positive granule neurons were identified based on their distinctive somal size and bifurcating "T"-shaped parallel fiber axons (Figure 1J). Granule neurons in the internal granular layer (IGL) in S5a/Rpn10 knockdown animals had shorter dendrites with reduced dendrite branching than IGL granule neurons in control animals (Figure 1K). Quantitation revealed a decrease in the number of secondary and tertiary dendrite branches and a 2-fold reduction in total dendrite length in IGL neurons in S5a/Rpn10 knockdown animals (Figures 1L–1N). S5a/Rpn10 knockdown had little or no effect on parallel fiber patterning or the number of parallel fibers associated with IGL granule neurons (data not shown). Together, these data indicate a cell-autonomous role for

morphology, arrows and arrowheads indicate dendrites and axons, respectively. S5a/Rpn10 knockdown led to shorter, less branched dendrites. The scale bar represents 10 μm.

(E) Total dendrite length for granule neurons treated as in (D) was quantified. These data and subsequent histogram data are presented as mean + SEM. Total dendrite length was significantly reduced in S5a/Rpn10 knockdown neurons compared to control U6- and scrambled S5a/Rpn10 RNAi-transfected neurons (ANOVA; p < 0.005; 450 neurons).

(F) Lysates of 293T cells transfected with a plasmid encoding GFP-S5a-WT or GFP-S5a-RES together with the S5a/Rpn10 RNAi or control U6 plasmid were immunoblotted with indicated antibodies.

(G) Granule neurons transfected with the S5a/Rpn10 RNAi or control U6 plasmid together with the S5a-WT or S5a-RES plasmids or control vector and the GFP plasmid were analyzed as in (D). S5a-RES but not S5a-WT increased granule neuron dendrite growth and elaboration compared to control vector in the background of S5a/Rpn10 RNAi. The scale bar represents 10 μm.

(H) Total dendrite length for granule neurons treated as in (G) was quantified. S5a-RES but not S5a-WT significantly increased total dendrite length compared to control vector in the background of S5a/Rpn10 RNAi (ANOVA; p < 0.005; 360 neurons).

(I) Granule neurons transfected with a plasmid encoding full-length S5a/Rpn10 (S5a), a dominant negative form of S5a/Rpn10 that lacks the N terminus (S5aC), or control vector were analyzed as in (D). Total dendrite length was significantly increased in S5a/Rpn10-transfected neurons compared to control vector-transfected neurons. Total dendrite length was significantly reduced in neurons expressing S5aC compared to control-vector transfected neurons (ANOVA; p < 0.005, 270 neurons).

(J) Rat pups electroporated in vivo with a U6-S5ai/CMV-GFP RNAi or control U6/CMV-GFP plasmid were sacrificed 5 days after electroporation (P8) and cerebella were subjected to immunohistochemistry using GFP and Calbindin antibodies. Representative control-transfected granule neurons are shown with their somas (asterisks) and dendrites in the IGL and ascending axons (arrowheads) connecting to horizontally oriented parallel fibers superficially. The scale bar represents 10 μm.

(K) Rat pups were electroporated as in (J), and a representative neuron for each condition is shown. IGL granule neurons in S5a/Rpn10 knockdown animals had shorter, less branched dendrites than IGL granule neurons in control U6 animals. The scale bar represents 10 μm.

(L–N) IGL granule neurons in vivo treated as in (K) were subjected to morphometric analysis. Total dendrite length (L), primary dendrite number (M), and secondary and tertiary dendrite branch number (N) were significantly reduced in IGL granule neurons in S5a/Rpn10 knockdown animals compared to control U6 animals (ANOVA, p < 0.0001, 270 neurons).
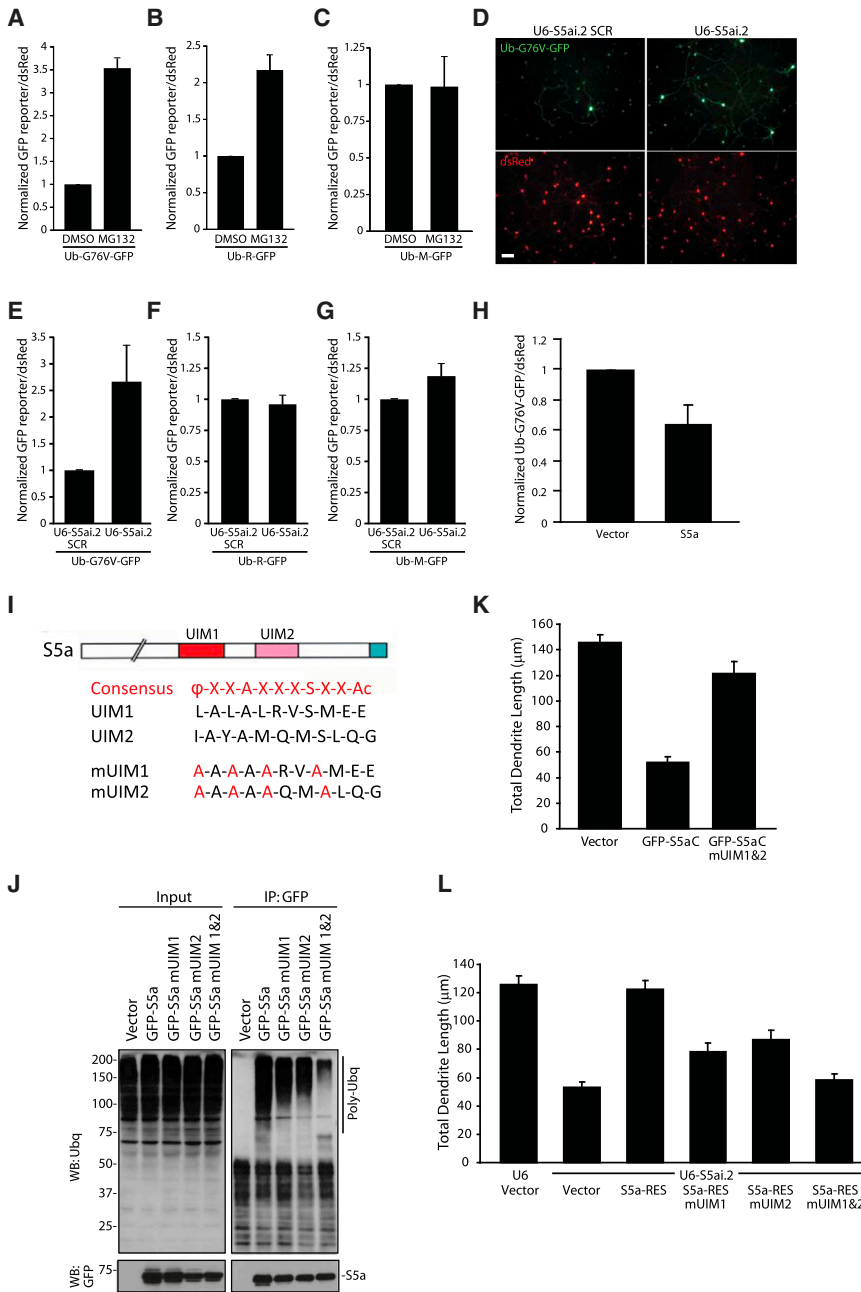
Figure 2. S5a/Rpn10 Regulates Proteasomal Degradation of Ubiquitin Conjugates in Neurons

(A–C) Lysates of granule neurons transfected with a plasmid encoding Ub-G76V-GFP (A), Ub-R-GFP (B), or Ub-M-GFP (C) together with a plasmid encoding dsRed and treated with MG132 or control DMSO for 18 hr were analyzed by fluorometry. GFP fluorescence values were normalized to dsRed fluorescence. The relative amount of Ub-G76V-GFP or Ub-R-GFP but not Ub-M-GFP was significantly increased in MG132-treated neurons compared to control DMSO treatment (Kruskal-Wallis; $p < 0.01$; n = 4).

(D) Granule neurons transfected with S5a/Rpn10 RNAi (U6-S5ai) or control scrambled S5a/Rpn10 RNAi (U6-S5ai SCR) and the Ub-G76V-GFP and dsRed plasmids were subjected to live fluorescence microscopy 2 days later. Representative fields are shown. S5a/Rpn10 knockdown increased the abundance of Ub-G76V-GFP with little or no effect on dsRed expression. The scale bar represents 50 μm.

(E–G) Lysates of granule neurons transfected with the Ub-G76V-GFP (E), Ub-R-GFP (F), or Ub-M-GFP (G) plasmid together with the dsRed plasmid and S5a/Rpn10 RNAi (U6-S5ai) or control scrambled S5a/Rpn10 RNAi (U6-S5ai SCR) were analyzed by fluorometry as in (A). The relative abundance of Ub-G76V-GFP but not Ub-R-GFP or Ub-M-GFP was significantly increased in S5a/Rpn10 knockdown neurons compared to control scrambled S5a/Rpn10 RNAi-transfected neurons (Kruskal-Wallis; $p < 0.05$; n = 3).

(H) Granule neurons transfected with S5a/Rpn10 or control vector and the Ub-G76V-GFP and dsRed plasmids were analyzed by fluorometry as in (A). The relative abundance of Ub-G76V-GFP was significantly reduced in S5a/Rpn10-expressing neurons compared to control vector-transfected neurons (Kruskal-Wallis; $p < 0.05$; n = 3).

(I) Schematic of S5a/Rpn10 domain structure and UIM consensus motif with corresponding mutants for the UIM domains as shown (Young et al., 1998).

(J) Lysates of 293T cells transfected with the GFP-S5a, GFP-S5a mUIM1, GFP-S5a mUIM2, GFP-S5a mUIM1&2, or control vector were immunoprecipitated using the GFP antibody and immunoblotted with indicated antibodies. Mutation of the UIM domains reduced the interaction between S5a/Rpn10 and ubiquitin conjugates.

(K) Granule neurons transfected with the GFP-S5aC plasmid, a plasmid encoding GFP-S5aC mUIM1&2, or control vector were analyzed as in Figure 1D. GFP-S5aC but not GFP-S5aC mUIM1&2 significantly reduced total dendrite length compared to control vector transfection (ANOVA, $p < 0.005$; 270 neurons).

(L) Granule neurons transfected with the S5a/Rpn10 RNAi or control U6 plasmid together with a plasmid encoding S5a-RES, S5a-RES mUIM1, S5a-RES mUIM2, S5a-RES mUIM1&2, or control vector and the GFP plasmid were analyzed as in (K). S5a-RES but not S5a-RES mUIM1, S5a-RES mUIM2, or S5a-RES mUIM1&2 significantly increased dendrite length compared to control vector in the background of S5a/Rpn10 RNAi (ANOVA; $p < 0.001$; 540 neurons).

S5a/Rpn10 in the elaboration of dendrite arbors in the cerebellar cortex in vivo.

S5a/Rpn10 Regulates Proteasome-Dependent Degradation of Ubiquitin Conjugates in Neurons

The identification of a role for S5a/Rpn10 in dendrite patterning led us to determine the molecular basis of S5a/Rpn10 function in neurons. We employed proteasomal reporters to characterize the role of S5a/Rpn10 in the regulation of proteasome function in neurons (Dantuma et al., 2000). First, we confirmed that the proteasomal inhibitor MG132 increased the abundance of the proteasome reporters Ub-R-GFP and Ub-G76V-GFP, which depend on N-end rule and UFD signals for degradation, respectively (Figures 2A and 2B; Johnson et al., 1992; Varshavsky,
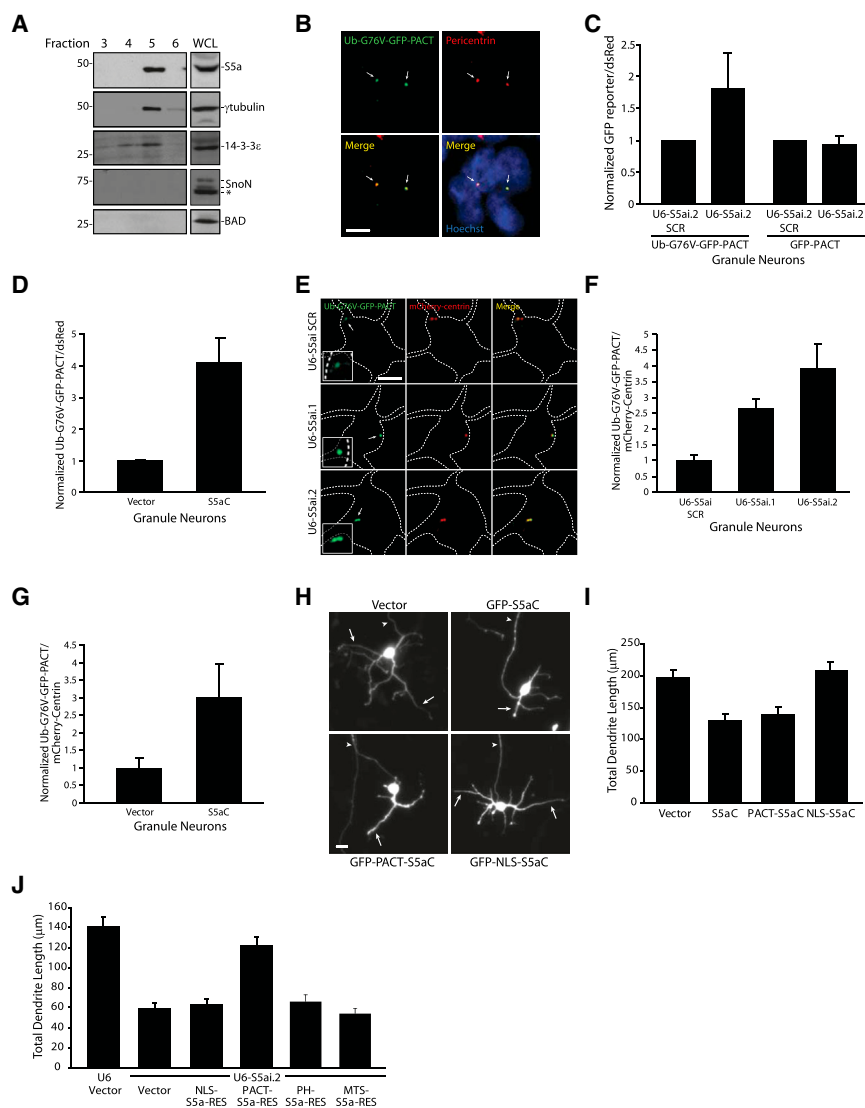
Figure 3. S5a/Rpn10 Acts Locally at the Centrosome to Regulate Proteasome Activity and Thereby Drives Dendrite Development in Mammalian Neurons

(A) Fractions isolated from a granule neuron centrosome preparation were immunoblotted using indicated antibodies. Whereas γ-tubulin and 14-3-3ε specifically identified centrosomal fractions, SnoN and BAD, which are found in the nucleus and cytosol, respectively, were absent from centrosomal fractions. Asterisk indicates nonspecific band. WCL, whole cell lysate.

(B) Granule neurons transfected with a plasmid encoding Ub-G76V-GFP-PACT were subjected to immunocytochemistry using GFP or Pericentrin antibodies. Representative neurons are shown. Arrows indicate the location of the centrosome based on Pericentrin immunofluorescence. Scale bar, 10 μm.

(C) Lysates of granule neurons transfected with S5a/Rpn10 RNAi (U6-S5ai) or control scrambled S5a/Rpn10 RNAi (U6-S5ai SCR) together with the Ub-G76V-GFP-PACT or GFP-PACT plasmids and dsRed plasmid were analyzed by fluorometry as in Figure 2A. The relative abundance of Ub-G76V-GFP-PACT but not GFP-PACT was significantly increased in S5a/Rpn10 knockdown neurons compared to control scrambled S5a/Rpn10 RNAi-transfected neurons (Kruskal-Wallis; $p < 0.05$; n = 3).

(D) Lysates of granule neurons transfected with the S5aC plasmid or control vector together with the Ub-G76V-GFP-PACT and dsRed plasmids were analyzed by fluorometry as in (C). The relative abundance of Ub-G76V-GFP-PACT was significantly increased in S5aC-trasfected neurons compared to control vector-transfected neurons (Kruskal-Wallis; $p < 0.05$; n = 3).

(E) Granule neurons transfected with S5a/Rpn10 RNAi (U6-S5ai) or control scrambled S5a/Rpn10 RNAi (U6-S5ai SCR) together with the Ub-G76V-GFP-PACT and mCherry-centrin plasmids were subjected to immunocytochemistry using GFP or dsRed antibody. S5a/Rpn10 knockdown substantially increased the abundance of Ub-G76V-

GFP-PACT with little or no effect on mCherry-centrin. Arrows indicate the location of the centrosome based on mCherry-centrin immunofluorescence. The scale bar represents 5 μm.

(F) GFP and mCherry fluorescence at the centrosome was quantified for granule neurons treated as in (E). The relative immunofluorescence of Ub-G76V-GFP-PACT at the centrosome was significantly increased in S5a/Rpn10 knockdown neurons compared to control scrambled S5a/Rpn10 RNAi-transfected neurons (Kruskal-Wallis; $p < 0.01$; 270 neurons).

(G) GFP and mCherry fluorescence at the centrosome was quantified for granule neurons transfected with the S5aC plasmid or control vector together with the Ub-G76V-GFP-PACT and mCherry-centrin plasmids as in (E). The relative immunofluorescence of Ub-G76V-GFP-PACT at the centrosome was significantly increased in S5aC-expressing neurons compared to control vector-transfected neurons (Kruskal-Wallis; $p < 0.01$; 180 neurons).

(H) Granule neurons transfected with the GFP-S5aC, GFP-PACT-S5aC, GFP-NLS-S5aC plasmid, or control vector were analyzed as in Figure 1D. GFP-S5aC and GFP-PACT-S5aC but not GFP-NLS-S5aC substantially reduced dendrite length.

(I) Total dendrite length for granule neurons treated as in (H) was quantified. Total dendrite length was significantly reduced in neurons transfected with GFP-S5aC and GFP-PACT-S5aC but not in neurons transfected with GFP-NLS-S5aC compared to control vector-transfected neurons (ANOVA; $p < 0.005$; 360 neurons).

(J) Granule neurons transfected with the S5a/Rpn10 RNAi or control U6 plasmid together with a plasmid encoding NLS-S5a-RES, PACT-S5a-RES, PH-S5a-RES, MTS-S5a-RES, or control vector and the GFP plasmid were analyzed as in (H). PACT-S5a-RES but not NLS-S5a-RES, PH-S5a-RES, or MTS-S5a-RES significantly increased dendrite length compared to control vector in the background of S5a/Rpn10 RNAi (ANOVA; $p < 0.01$; 480 neurons).

See also Figures S1 and S2.

1996). MG132 had little or no effect on the abundance of control fusion protein, Ub-M-GFP (Figure 2C). Importantly, knockdown of S5a/Rpn10 dramatically increased the abundance of the Ub-G76V-GFP reporter in neurons by immunofluorescence and quantitative fluorometric analyses (Figures 2D and 2E). Conversely, expression of S5a/Rpn10 reduced the abundance of the Ub-G76V-GFP reporter in neurons (Figure 2H). S5a/Rpn10 knockdown had little to no effect on the abundance of
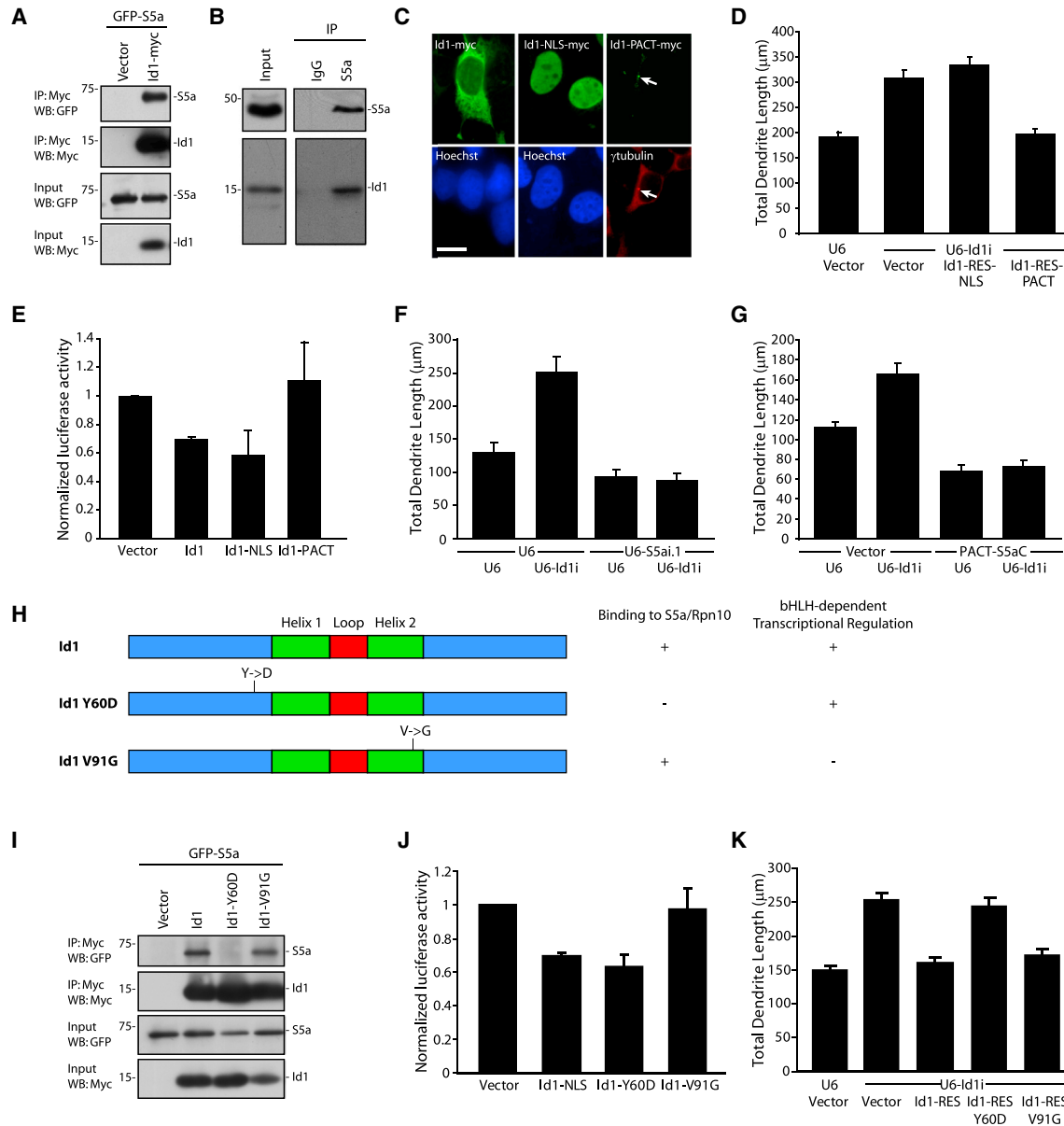
Figure 4. Id1 Suppresses S5a/Rpn10-Dependent Dendrite Morphogenesis

(A) Lysates of 293T cells transfected with the GFP-S5a plasmid together with a plasmid encoding Id1-myc were immunoprecipitated using the Myc antibody and immunoblotted with indicated antibodies.

(B) Lysates of granule neurons were immunoprecipitated with S5a/Rpn10 or control IgG antibodies and immunoblotted with indicated antibodies. Endogenous S5a/Rpn10 and Id1 interacted in granule neurons.

(C) 293T cells transfected with the Id1-myc, Id1-NLS-myc, or Id1-PACT-myc plasmid were subjected to immunocytochemistry using the Myc antibody and the γ-tubulin antibody to label centrosomes. DNA dye bisbenzimide (Hoechst) labels the nucleus. Arrows indicate colocalization of Id1-PACT-myc with γ-tubulin. The scale bar represents 5 μm.

(D) Granule neurons transfected with the Id1 RNAi (U6-Id1i) or control U6 plasmid together with a plasmid encoding Id1-NLS-RES, Id1-PACT-RES, or control vector and the GFP plasmid were analyzed as in Figure 1D. Id1-PACT-RES but not Id1-NLS-RES significantly reduced dendrite length compared to control vector in the background of Id1 RNAi (ANOVA; p < 0.0001; 360 neurons).

(E) Granule neurons transfected with a plasmid encoding Id1, Id1-NLS, Id1-PACT, or control vector together with plasmids encoding a bHLH-dependent pFOX promoter-driven luciferase reporter and Renilla were analyzed by luminometry. Luminescence values were normalized to Renilla to control for transfection efficiency. The relative amount of the pFOX-dependent luciferase reporter was significantly decreased in Id1- and Id1-NLS-transfected neurons but not Id1-PACT-transfected neurons compared to control vector-transfected neurons (Kruskal-Wallis; p < 0.01; n = 5).

(F) Granule neurons transfected with the Id1 RNAi or control U6 plasmid together with S5a RNAi or control U6 plasmid and the GFP plasmid were analyzed as in (D). Id1 knockdown significantly increased total dendrite length compared to control. S5a/Rpn10 RNAi significantly reduced total dendrite length in neurons in the presence or absence of Id1 knockdown (ANOVA, p < 0.0001; 360 neurons).

(legend continued on next page)

the N-end rule substrate Ub-R-GFP or the proteasome-resistant Ub-M-GFP reporter (Figures 2F and 2G). These data suggest that S5a/Rpn10 plays a critical role in the regulation of proteasome function through the UFD pathway in neurons.

We next determined the role of S5a/Rpn10-induced degradation of ubiquitin conjugates in dendrite morphogenesis. The ubiquitin interacting motifs (UIM) in S5a/Rpn10 are essential for S5a/Rpn10 function in the degradation of ubiquitin conjugates (Young et al., 1998). We confirmed that mutation of a critical conserved motif within the UIMs disrupted the ability of S5a/Rpn10 to bind ubiquitin conjugates in cells (Figures 2I and 2J). Mutation of the UIMs abrogated the ability of the dominant interfering S5a/Rpn10 mutant, S5aC, to inhibit dendrite elaboration in neurons (Figures 2I and 2K). Importantly, in structure-function analyses in the setting of S5a/Rpn10 RNAi, expression of S5a/Rpn10 rescue mutants in which one or both UIM domains are disrupted (S5a-RES mUIM1, S5a-RES mUIM2, and S5a-RES mUIM1&2) failed to restore dendrite elaboration in granule neurons (Figures 2I and 2L). Together, our data suggest S5a/Rpn10 promotes the degradation of ubiquitinated conjugates in neurons to drive dendrite morphogenesis.

S5a/Rpn10 Acts Locally at the Centrosome to Regulate Proteasome Activity and Thereby Drives Dendrite Development

The centrosome has recently emerged as a critical subcellular locale for the regulation of dendrite morphogenesis (Kim et al., 2009; Puram et al., 2011a; Yamada et al., 2013). We therefore asked whether S5a/Rpn10 might regulate proteasome function at the centrosome and thereby regulate dendrite development. In granule neuron lysates, a pool of endogenous S5a/Rpn10 cofractionated with the centrosomal proteins γ-tubulin and 14-3-3ε (Figure 3A). Consistent with these results, expression of a GFP-S5a/Rpn10 fusion protein revealed that a pool of S5a/Rpn10 colocalized with centrosomal marker Pericentrin (Figure S1). To test if S5a/Rpn10 promotes proteasome function at the centrosome, we used the Ub-G76V-GFP reporter protein fused at its C terminus to the PACT domain of AKAP450 (Gillingham and Munro, 2000), which localizes proteins to the centrosome (Ub-G76V-GFP-PACT) (Figure 3B). Strikingly, knockdown of S5a/Rpn10 increased the abundance of the centrosomal Ub-G76V-GFP-PACT reporter, but not the control GFP-PACT protein, in granule neurons by fluorometry (Figure 3C). Expression of the dominant interfering S5a/Rpn10 mutant, S5aC, also increased the abundance of the Ub-G76V-GFP-PACT reporter

in neurons (Figure 3D). Immunofluorescence analyses also revealed that inhibition of endogenous S5a/Rpn10 by knockdown or expression of S5aC increased the levels of the Ub-G76V-GFP-PACT reporter at the centrosome in neurons (Figures 3E–3G). Together, these data suggest S5a/Rpn10 stimulates the degradation of ubiquitin conjugates at the centrosome in mammalian brain neurons.

We next characterized the role of centrosomal S5a/Rpn10 in the regulation of dendrite morphogenesis. We first inhibited endogenous S5a/Rpn10 function at the centrosome by targeting S5aC to the centrosome via fusion to the PACT domain (PACT-S5aC). Remarkably, expression of PACT-S5aC in granule neurons reduced dendrite length as effectively as S5aC (Figures 3H and 3I). In contrast, expression of a nuclearly localized form of S5aC (NLS-S5aC) had little or no effect on dendrite elaboration (Figures 3H and I). In structure-function analyses of S5a/Rpn10 in the setting of RNAi, expression of PACT-S5a-RES robustly induced dendrite growth, suggesting that S5a/Rpn10 forcibly localized to the centrosome can drive dendrite elaboration in neurons (Figure 3J). In contrast, S5a-RES localized in the nucleus (NLS-S5a-RES), at the plasma membrane (PH-S5a-RES), or the mitochondrial membrane (MTS-S5a-RES) failed to promote dendrite growth in the background of S5a/Rpn10 RNAi in granule neurons (Figures 3J and S2). Together, these results suggest S5a/Rpn10 specifically operates at the centrosome to drive dendrite morphogenesis in neurons.

The Helix-Loop-Helix Protein Id1 Suppresses S5a/Rpn10-Dependent Dendrite Morphogenesis

The identification of a function for proteasomes at the centrosome in the control of dendrite development led us to the question of how this function is regulated in neurons. In yeast-two hybrid assays, S5a/Rpn10 interacts with the helix-loop-helix (HLH) protein Id1 (Anand et al., 1997). Although Id1 inhibits the function of basic HLH (bHLH) transcription factors in the nucleus, Id1 is also present at the centrosome and inhibits dendrite growth and elaboration in neurons (Kim et al., 2009). These observations raised the question of whether Id1 regulates centrosomal S5a/Rpn10 function in dendrite morphogenesis.

We first confirmed that Id1 and S5a/Rpn10 interact in cells (Figure 4A). Importantly, endogenous Id1 interacted with endogenous S5a/Rpn10 in neurons (Figure 4B). In view of Id1's function in the regulation of transcription, we next asked whether Id1 acts at the centrosome or nucleus to control dendrite growth. Expression of an RNAi-resistant mutant Id1 localized to the centrosome

---

(G) Granule neurons transfected with the Id1 RNAi or control U6 plasmid together with the PACT-S5aC plasmid or control vector and the GFP plasmid were analyzed as in (D). Id1 knockdown significantly increased total dendrite length compared to control. Expression of PACT-S5aC significantly reduced total dendrite length in neurons in the presence or absence of Id1 knockdown (ANOVA, p < 0.0001; 360 neurons).

(H) Schematic of Id1 point mutants used in structure-function analyses of Id1.

(I) Lysates of 293T cells transfected with the GFP-S5a plasmid together with a plasmid encoding Id1-myc, Id1-Y60D-myc, Id1-V91G-myc, or control vector were immunoprecipitated using the Myc antibody and immunoblotted with indicated antibodies. Tyrosine 60 (Y60) is required for Id1 interaction with S5a/Rpn10, whereas valine 91 (V91) is dispensable for Id1 interaction with S5a/Rpn10.

(J) Granule neurons transfected with the plasmid encoding Id1-NLS, Id1-Y60D, Id1-V91G, or control vector together with the pFOX luciferase reporter and Renilla plasmids were analyzed as in (E). The relative amount of the pFOX luciferase reporter was significantly decreased in Id1-NLS and Id1-Y60D-transfected neurons but not Id1-V91G-transfected neurons compared to control vector-transfected neurons (Kruskal-Wallis; p < 0.05; n = 3).

(K) Granule neurons transfected with the Id1 RNAi or control U6 plasmid together with a plasmid encoding Id1-RES, Id1-RES-Y60D, Id1-RES-V91G, or control vector and the GFP plasmid were analyzed as in (D). Id1-RES and Id1-RES-V91G but not Id1-RES-Y60D significantly reduced dendrite length compared to control vector in the background of Id1 RNAi (ANOVA; p < 0.001; 450 neurons).
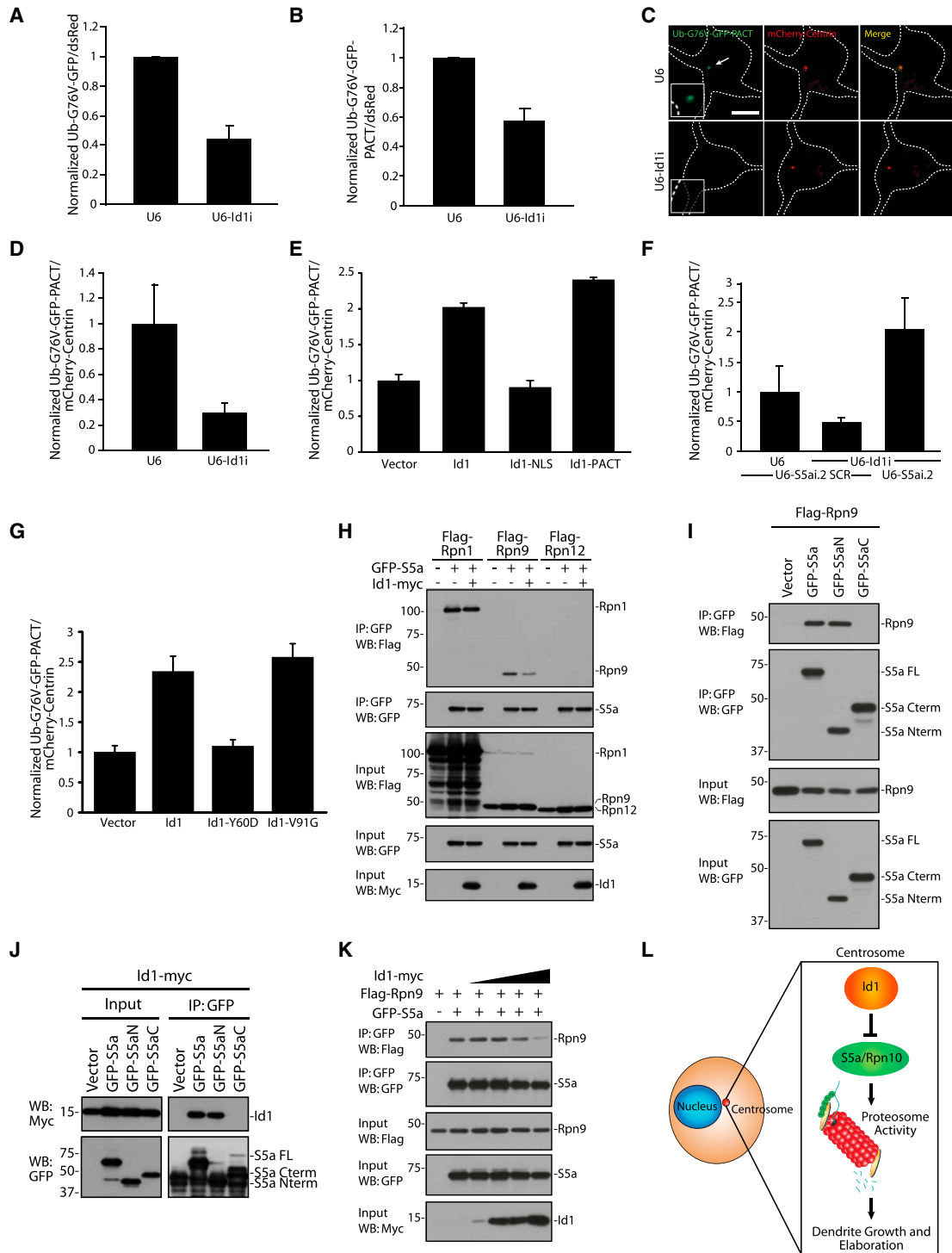
Figure 5. Id1 Disrupts S5a/Rpn10 Binding to the Proteasome Lid and Thereby Reduces S5a/Rpn10-Dependent Degradation of Ubiquitinated Conjugates at the Centrosome

(A) Granule neurons transfected with Id1 RNAi or control U6 plasmid and the Ub-G76V-GFP and dsRed plasmids were analyzed by fluorometry as in Figure 2A. The relative abundance of Ub-G76V-GFP was significantly reduced in Id1 knockdown neurons compared to control U6-transfected neurons (Kruskal-Wallis; p < 0.05; n = 3).

(B) Granule neurons transfected with Id1 RNAi (U6-Id1i) or control U6 plasmid and the Ub-G76V-PACT-GFP and dsRed plasmids were analyzed by fluorometry as in (A). The relative abundance of Ub-G76V-GFP-PACT was significantly reduced in Id1 knockdown neurons compared to control U6-transfected neurons (Kruskal-Wallis; p < 0.05; n = 3).

(legend continued on next page)

(Id1-RES-PACT) but not the nucleus (Id1-RES-NLS) inhibited dendrite growth in the setting of Id1 RNAi in neurons (Figures 4C and 4D). In control experiments, expression of Id1 and nuclearly localized Id1 but not centrosomally localized Id1 inhibited bHLH-dependent transcription in neurons (Figure 4E). Together, these data suggest Id1 regulates dendrite development from its subcellular localization at the centrosome and independently of its effects on bHLH-dependent transcription.

We next evaluated the relationship between Id1 and S5a/Rpn10 in dendrite morphogenesis. Knockdown of S5a/Rpn10 and expression of the centrosomally localized dominant interfering mutant of S5a/Rpn10 (PACT-S5aC) reduced dendrite length in the presence or absence of Id1 RNAi, suggesting S5a/Rpn10 lies downstream of Id1 (Figures 4F and 4G). To characterize the functional consequences of Id1 binding to S5a/Rpn10, we employed a structure-function approach with Id1 mutants in granule neurons (Figure 4H). A mutation of Id1 at Tyrosine 60 (Y60D), a residue that is N-terminal to the HLH domain, disrupted Id1 binding to S5a/Rpn10 (Figure 4I) but had little or no effect on Id1-inhibition of bHLH-dependent transcription (Figure 4J). A mutation of Id1 at Valine 91 (V91G), which lies in the second α helix of the HLH domain, impaired the ability of Id1 to inhibit bHLH-dependent transcription (Figure 4J) but had little or no effect on Id1 binding to S5a/Rpn10 (Figure 4I). These mutations of Id1 facilitated characterization of the role of Id1 binding to S5a/Rpn10 as well as Id1-inhibition of bHLH-dependent transcription in dendrite development. In morphology assays, the Id1-RES V91G mutant but not the Id1-RES Y60D mutant inhibited dendrite growth in neurons in the background of Id1 RNAi (Figure 4K). Together, these results suggest Id1 forms a complex with S5a/Rpn10 and thereby regulates dendrite development in mammalian neurons independently of its function in bHLH-dependent transcriptional regulation.

Id1 Disrupts S5a/Rpn10 Binding to the Proteasome Lid and Thereby Reduces S5a/Rpn10-Dependent Degradation of Centrosomal Ubiquitinated Conjugates

The findings that centrosomal Id1 regulates dendrites via its interaction with S5a/Rpn10 and independently of bHLH transcription raised the possibility that Id1 might regulate proteasome function at the centrosome and thereby control dendrite patterning. Knockdown of Id1 in granule neurons reduced the abundance of the Ub-G76V-GFP reporter (Figure 5A), suggesting that Id1 inhibits proteasome function. Importantly, in fluorometric and immunofluorescence analyses, Id1 knockdown reduced and expression of Id1 increased the levels of the Ub-G76V-GFP-PACT reporter in granule neurons (Figures 5B–5E). We also found that centrosomally localized Id1 (Id1-PACT) but not nuclearly localized Id1 (Id1-NLS) increased the abundance of the Ub-G76V-GFP-PACT reporter (Figure 5E). These data suggest that Id1 inhibits the degradation of ubiquitin conjugates at the centrosome.

How might Id1 exert its function at the centrosome and inhibit proteasomal activity? In light of the biochemical interaction between Id1 and S5a/Rpn10 (Figures 4A and 4B; Anand et al., 1997), we first defined the genetic relationship between Id1 and S5a/Rpn10 in the regulation of proteasome activity in neurons. In epistasis analyses, the Id1 knockdown-induced reduction in Ub-G76V-GFP-PACT abundance was suppressed by S5a/Rpn10 knockdown (Figure 5F), suggesting that Id1 operates upstream of S5a/Rpn10 in regulating proteasomal activity at the centrosome. Accordingly, Id1 Y60D, which failed to bind S5a/Rpn10 (Figure 4I), had little or no effect on the abundance of

(C) Granule neurons transfected with Id1i RNAi or control U6 plasmid together with the Ub-G76V-GFP-PACT and mCherry-centrin plasmids were analyzed as in Figure 3E. Id1 knockdown substantially decreased the abundance of Ub-G76V-GFP-PACT with little or no effect on mCherry-centrin. The scale bar represents 5 μm.

(D) GFP and mCherry fluorescence at the centrosome was quantified for granule neurons treated as in (C). The relative immunofluorescence of Ub-G76V-GFP-PACT at the centrosome was significantly decreased in Id1 knockdown neurons compared to control U6-transfected neurons (Kruskal-Wallis; p < 0.01; 180 neurons).

(E) GFP and mCherry fluorescence at the centrosome was quantified in granule neurons transfected with Id1, Id1-NLS, Id1-PACT, or control vector together with the Ub-G76V-GFP-PACT and mCherry-centrin plasmids as in (C). Whereas Id1 and Id1-PACT significantly increased the relative immunofluorescence of Ub-G76V-GFP-PACT compared to control transfected neurons, Id1-NLS had little or no effect on the relative immunofluorescence of Ub-G76V-GFP-PACT compared to control neurons (Kruskal-Wallis; p < 0.01; 360 neurons).

(F) GFP and mCherry fluorescence at the centrosome was quantified for granule neurons transfected with the Id1 RNAi or control U6 plasmid together with the S5a/Rpn10 RNAi or control scrambled S5a/Rpn10 RNAi plasmid and the Ub-G76V-GFP-PACT and mCherry-centrin plasmids as in (C). Whereas Id1 RNAi significantly decreased the relative immunofluorescence of Ub-G76V-GFP-PACT compared to control transfected neurons, S5a/Rpn10 RNAi significantly increased the relative immunofluorescence of Ub-G76V-GFP-PACT in the background of Id1 knockdown compared to control neurons (Kruskal-Wallis; p < 0.01, 270).

(G) GFP and mCherry fluorescence at the centrosome was quantified in granule neurons transfected with Id1, Id1-Y60D, Id1-V91G, or control vector together with the Ub-G76V-GFP-PACT and mCherry-centrin plasmids as in (C). Whereas Id1 and Id1-V91G significantly increased the relative immunofluorescence of Ub-G76V-GFP-PACT compared to control transfected neurons, Id1-Y60D had little or no effect on the relative immunofluorescence of Ub-G76V-GFP-PACT compared to control neurons (Kruskal-Wallis; p < 0.01; 206 neurons).

(H) Lysates of 293T cells transfected with a plasmid encoding Flag-Rpn1, Flag-Rpn9, or Flag-Rpn12 together with the GFP-S5a plasmid or control vector and the Id1-myc plasmid or control vector were immunoprecipitated using the GFP antibody and immunoblotted with indicated antibodies.

(I) Lysates of 293T cells transfected with the Flag-Rpn9 plasmid together with a plasmid encoding full-length S5a/Rpn10 (GFP-S5a), N-terminal S5a/Rpn10 (GFP-S5aN), C-terminal S5a/Rpn10 (GFP-S5aC), or control vector were immunoprecipitated using the GFP antibody and immunoblotted with indicated antibodies.

(J) Lysates of 293T cells transfected with the Id1-myc plasmid together with the plasmid encoding GFP-S5a, GFP-S5aN, GFP-S5aC, or control vector were immunoprecipitated using the GFP antibody and immunoblotted with indicated antibodies.

(K) Lysates of 293T cells transfected with the Flag-Rpn9 plasmid together with the GFP-S5a plasmid or control vector and increasing amounts of the Id1-myc plasmid were immunoprecipitated using the GFP antibody and immunoblotted with indicated antibodies.

(L) Model of the Id1-regulated centrosomal S5a/Rpn10 signaling pathway that drives dendrite growth and elaboration in the mammalian brain.

the centrosomal Ub-G76V-GFP-PACT reporter (Figure 5G). By contrast, Id1 V91G, which binds to S5a/Rpn10 but failed to regulate bHLH-dependent transcription (Figures 4I and 4J), increased the abundance of the Ub-G76V-GFP-PACT reporter (Figure 5G), suggesting S5a/Rpn10 binding is critical for the ability of Id1 to inhibit centrosomal proteasome activity in neurons. Together, these data suggest Id1 inhibits S5a/Rpn10-dependent degradation of ubiquitin conjugates at the centrosome.

We next characterized a mechanism by which Id1 disrupts S5a/Rpn10-dependent degradation of centrosomal ubiquitin conjugates. Because S5a/Rpn10 binds to components of the proteasomal lid and traffics ubiquitin conjugates to the proteasome (Deveraux et al., 1994; van Nocker et al., 1996; Verma et al., 2004), we asked if Id1 disrupts S5a/Rpn10 binding to proteasomal lid proteins and thereby interferes with degradation of S5a/Rpn10-bound substrates. We first assessed the ability of S5a/Rpn10 to form a complex with the lid proteins Rpn1, Rpn9, and Rpn12, which are reported to form a complex with S5a/Rpn10 in yeast or in vitro (Riedinger et al., 2010; Rosenzweig et al., 2012; Takeuchi et al., 1999). These analyses revealed that S5a/Rpn10 robustly forms a complex with Rpn1 and Rpn9 but not Rpn12 in cells (Figure 5H). Interestingly, expression of Id1 inhibited the interaction of S5a/Rpn10 with Rpn9 (Figure 5H).

To determine the mechanism by which Id1 inhibits the interaction of S5a/Rpn10 with Rpn9, we first mapped the interactions of S5a/Rpn10 with Rpn9 and with Id1. Deletion of the N terminus of S5a/Rpn10 impaired the ability of S5a/Rpn10 to form a complex with Rpn9 (Figure 5I). The N-terminal domain of S5a/Rpn10 was also required for its interaction with Id1 (Figure 5J). These results suggest Id1 might compete with Rpn9 to interact with S5a/Rpn10. Consistent with this prediction, expression of Id1 disrupted the S5a/Rpn10-Rpn9 interaction in a dose-dependent manner in cells (Figure 5K). Together, these data suggest that Id1 inhibits S5a/Rpn10-dependent proteasomal function at the centrosome by interfering with the interaction of S5a/Rpn10 with the proteasomal lid protein Rpn9. Collectively, we have elucidated an Id1-regulated centrosomal S5a/Rpn10 signaling mechanism that drives the growth and elaboration of dendrite arbors in the mammalian brain (see model in Figure 5L).

DISCUSSION

In this study, we have discovered a function for proteasomes localized at the centrosome in neurons. Remarkably, although the ubiquitin receptor S5a/Rpn10 is distributed throughout the cell, a specific pool of S5a/Rpn10 is required for proteasome function at neuronal centrosomes to drive dendrite morphogenesis. We have also elucidated a critical mechanism that regulates proteasome function at the centrosome in neurons, whereby the HLH protein Id1 directly binds S5a/Rpn10 to suppress centrosomal proteasome function and thereby control dendrite patterning.

The identification of a function for proteasomes at the centrosome in neurons bears important ramifications for our understanding of proteasome function in general biological processes. Beyond the control of dendrite morphogenesis, signaling at the centrosome is thought to regulate diverse biological events, from migration in neurons to ciliogenesis to polarized

secretion in immune cells (Bornens, 2012; Griffiths et al., 2010). Therefore, our findings suggest centrosomal proteasome function plays a critical role in the regulation of distinct developmental and homeostatic processes in multicellular organisms.

Our findings suggest S5a/Rpn10 promotes the degradation of UFD pathway substrates to drive dendrite development, raising the intriguing possibility that centrosomal UFD pathway substrates may represent specific regulators of neuronal morphogenesis. In the future, it will be important to identify specific substrates of the centrosomal proteasome that control dendrite morphogenesis.

The signals acting upstream of S5a/Rpn10 in higher-order eukaryotes have remained elusive. Previous studies have described an interaction between Id1 and S5a/Rpn10 in nonneural cells (Anand et al., 1997; Hasskarl et al., 2008), but the physiological effects of this interaction remained unknown. In this study, we have found that the HLH protein Id1 interacts with S5a/Rpn10 in neurons and thereby inhibits centrosomal proteasome function. Id1 also localizes in the nucleus (Benezra et al., 1990), raising the possibility that, in addition to inhibiting bHLH transcription factors, Id1 may regulate the proteasome in the nucleus. At the centrosome in neurons, Id1 operates independently of its canonical role in the regulation of transcription to restrain dendrite development by suppressing S5a/Rpn10 binding to core proteasome lid proteins. Elucidation of the regulation of Id1-S5a/Rpn10 binding will further define the rules that control proteasome signaling and potentially lead to the design of drugs for human diseases, including cognitive disorders, in which manipulation of proteasome activity may be of therapeutic benefit.

EXPERIMENTAL PROCEDURES

Antibodies
Rabbit S5a/Rpn10 antibody (Thermo Scientific), rabbit and mouse GFP antibodies (Invitrogen), rabbit immunoglobulin G (IgG) (Upstate), rabbit Pericentrin antibody (Covance), and rabbit dsRed (Clontech) were purchased. Rabbit BAD, mouse Myc, mouse Actin, rabbit Id1, and rabbit SnoN were purchased from Santa Cruz Biotechnology. Mouse Flag, γ-tubulin, and Calbindin antibodies were purchased from Sigma. Rabbit 14-3-3ε antibody was a generous gift from Dr. Alastair Aitken (University of Edinburgh).

Plasmids
Rat S5a/Rpn10, Rpn1, Rpn9, and Rpn12 were cloned from rat granule neuron cDNA by PCR. S5a/Rpn10 was cloned into pEGFP-C1 (Clontech) to produce an N-terminal GFP-tagged S5a/Rpn10 expression plasmid. Expression plasmids for C-terminally Myc-tagged Id1 have been described (Kim et al., 2009). Rat Rpn1, Rpn9, and Rpn12 were cloned into p3XFlag-CMV-10 (Sigma) to produce Flag-tagged expression plasmids. Ub-M-GFP, Ub-R-GFP, and Ub-G76V-GFP (Addgene) and monomeric dsRed (Clontech) were purchased. The mCherry-centrin expression plasmid was generated by subcloning centrin from the GFP-centrin expression plasmid into the mCherry expression plasmid (Puram et al., 2011b). The pFox-luc reporter plasmid was a generous gift from Dr. Michael S. German (University of California, San Francisco).

RNAi plasmids were produced by insertion of the following oligonucleotides into pBS/U6 or pBS/U6-CMV-GFP: U6-S5ai.1: 5′-GGC AAG AAT CAC AAG ATG CGC CAAGTTAAC CCG CAT CTT GTG ATT CTT GCC CTTTTTG; U6-S5ai.2: 5′-TTG GGG AAG AGG AGG TGA ACT CAAGTTAAC TGT TCA CCT CCT CTT CCC CAA CTTTTTG; U6-Id1i has been described (Kim et al., 2009). RNAi-resistant (RES) expression plasmids to generate GFP-tagged S5a/Rpn10 (against U6-S5ai.2) and Id1-myc were produced by Quikchange mutagenesis (Stratagene) with silent mutations in the underlined

nucleotides: S5a/Rpn10: TCGGCGAGGAAGAAGTCAATA; Id1: GTAATTGATTATATTCGCGAT.

Subcellular localization-specific S5a/Rpn10, Id1, and Ub-G76V-GFP expression plasmids were generated as described (Kanaji et al., 2000; Kim et al., 2009; Stauffer et al., 1998). The human TOMM20 mitochondrial targeting sequence (MTS) plasmid was a generous gift from Dr. Jeff Milbrandt (Washington University). Mutations in S5a/Rpn10 and Id1 expression plasmids were generated using site-directed mutagenesis. S5a/Rpn10 N- (amino acids 1-195) and C-terminal (amino acids 196-377) mutants were created by PCR subcloning.

Primary Neuron Cultures and Transfection

Primary cerebellar granule neurons were prepared from P6 rat pups as described (Puram et al., 2011a) and were transfected as described (Konishi et al., 2004). The expression plasmid encoding the antiapoptotic protein Bcl-xl was included in all neuronal transfections. Expression of Bcl-xl had little or no effect on dendrite or axon morphology (data not shown; Gaudillière et al., 2004).

In Vivo Electroporation

All experiments using live animals have been approved by the Harvard Medical School Standing Committee on Animals and strictly conform to their regulatory standards. In vivo electroporation of P3 Sprague-Dawley rat pups was performed as described (Konishi et al., 2004).

Immunocytochemistry

For visualization of centrosomal proteins, cells were fixed in absolute methanol for 10 min at $-20°C$ and subjected to immunofluorescence analysis with indicated antibodies according to standard protocols. For other immunocytochemistry experiments, cells were fixed in 4% paraformaldehyde for 20 min at room temperature and analyzed as described (Konishi et al., 2004).

Immunoprecipitation and Centrosomal Fractionation

Immunoprecipitations of cell lysates were performed as described (Puram et al., 2011a), resolved by SDS-PAGE, and transferred to a nitrocellulose membrane for immunoblot analysis. Centrosomal fractions from granule neurons were isolated as described (Bornens et al., 1987).

Ubiquitin Reporter Assays

For quantitative fluorometric assays, GFP-tagged ubiquitin expression plasmids were transfected with dsRed and the indicated expression or RNAi plasmid in neurons as described (Kim et al., 2009). One or four days later, respectively, neurons were lysed using passive lysis buffer (Promega). Clarified lysates were analyzed by fluorometry for GFP and dsRed signal (Beckmann-Coulter). For quantitative immunocytochemistry, neurons were transfected with Ub-G76V-GFP-PACT and mCherry-centrin with the indicated RNAi or expression plasmid. Four days later, neurons were fixed and stained and GFP and mCherry fluorescence at the centrosome was quantified using National Institutes of Health ImageJ. Centrosomal mCherry fluorescence was similar across all conditions. For both quantitative fluorometric assays and immunocytochemical analyses, the background signal was subtracted, and the GFP signal was divided by the Cy3 channel signal to yield the normalized ubiquitin GFP reporter signal.

Luciferase Reporter Assays

The pFox-luciferase plasmid was transfected with the indicated expression plasmid or control vector in neurons as described (Kim et al., 2009). Four days later, luciferase and Renilla measurements were performed by luminometry (Promega).

Analysis of Neuronal Morphology and Imaging

Neuronal morphology of primary neurons and in vivo were performed as described (Gaudillière et al., 2004; Kim et al., 2009).

Statistics

Statistical analyses were performed with GraphPad Prism 4.0. All histograms are presented as mean + SEM unless otherwise noted. A two-tailed Student's t test was used for comparison of two sample groups comprised of parametric data. In experiments with more than two sample groups, ANOVA was performed followed by Bonferroni's post hoc test. For nonparametric data with more than two sample groups, the Kruskal-Wallis test was used.

REFERENCES

Anand, G., Yin, X., Shahidi, A.K., Grove, L., and Prochownik, E.V. (1997). Novel regulation of the helix-loop-helix protein Id1 by S5a, a subunit of the 26 S proteasome. J. Biol. Chem. 272, 19140–19151.

Benezra, R., Davis, R.L., Lockshon, D., Turner, D.L., and Weintraub, H. (1990). The protein Id: a negative regulator of helix-loop-helix DNA binding proteins. Cell 61, 49–59.

Besche, H.C., Peth, A., and Goldberg, A.L. (2009). Getting to first base in proteasome assembly. Cell 138, 25–28.

Bingol, B., Wang, C.F., Arnott, D., Cheng, D., Peng, J., and Sheng, M. (2010). Autophosphorylated CaMKIIalpha acts as a scaffold to recruit proteasomes to dendritic spines. Cell 140, 567–578.

Bornens, M. (2012). The centrosome in cells and organisms. Science 335, 422–426.

Bornens, M., Paintrand, M., Berges, J., Marty, M.C., and Karsenti, E. (1987). Structural and chemical characterization of isolated centrosomes. Cell Motil. Cytoskeleton 8, 238–249.

Dantuma, N.P., Lindsten, K., Glas, R., Jellne, M., and Masucci, M.G. (2000). Short-lived green fluorescent proteins for quantifying ubiquitin/proteasome-dependent proteolysis in living cells. Nat. Biotechnol. 18, 538–543.

Deveraux, Q., Ustrell, V., Pickart, C., and Rechsteiner, M. (1994). A 26 S protease subunit that binds ubiquitin conjugates. J. Biol. Chem. 269, 7059–7061.

Djakovic, S.N., Schwarz, L.A., DeMartino, G.N., and Patrick, G.N. (2009). Regulation of the proteasome by neuronal activity and calcium/calmodulin-dependent protein kinase II. J. Biol. Chem. 284, 26655–26665.

Fu, H., Reis, N., Lee, Y., Glickman, M.H., and Vierstra, R.D. (2001). Subunit interaction maps for the regulatory particle of the 26S proteasome and the COP9 signalosome. EMBO J. 20, 7096–7107.

Gaudillière, B., Konishi, Y., de la Iglesia, N., Yao, Gl., and Bonni, A. (2004). A CaMKII-NeuroD signaling pathway specifies dendritic morphogenesis. Neuron 41, 229–241.

Gillingham, A.K., and Munro, S. (2000). The PACT domain, a conserved centrosomal targeting motif in the coiled-coil proteins AKAP450 and pericentrin. EMBO Rep. 1, 524–529.

Griffiths, G.M., Tsun, A., and Stinchcombe, J.C. (2010). The immunological synapse: a focal point for endocytosis and exocytosis. J. Cell Biol. 189, 399–406.

Hasskarl, J., Mern, D.S., and Münger, K. (2008). Interference of the dominant negative helix-loop-helix protein ID1 with the proteasomal subunit S5A causes centrosomal abnormalities. Oncogene 27, 1657–1664.

Hatten, M.E., and Heintz, N. (1995). Mechanisms of neural patterning and specification in the developing cerebellum. Annu. Rev. Neurosci. *18*, 385–408.

Hershko, A., and Ciechanover, A. (1998). The ubiquitin system. Annu. Rev. Biochem. *67*, 425–479.

Johnson, E.S., Bartel, B., Seufert, W., and Varshavsky, A. (1992). Ubiquitin as a degradation signal. EMBO J. *11*, 497–505.

Kanaji, S., Iwahashi, J., Kida, Y., Sakaguchi, M., and Mihara, K. (2000). Characterization of the signal that directs Tom20 to the mitochondrial outer membrane. J. Cell Biol. *151*, 277–288.

Kim, A.H., Puram, S.V., Bilimoria, P.M., Ikeuchi, Y., Keough, S., Wong, M., Rowitch, D., and Bonni, A. (2009). A centrosomal Cdc20-APC pathway controls dendrite morphogenesis in postmitotic neurons. Cell *136*, 322–336.

Konishi, Y., Stegmüller, J., Matsuda, T., Bonni, S., and Bonni, A. (2004). Cdh1-APC controls axonal growth and patterning in the mammalian brain. Science *303*, 1026–1030.

Mabb, A.M., and Ehlers, M.D. (2010). Ubiquitination in postsynaptic function and plasticity. Annu. Rev. Cell Dev. Biol. *26*, 179–210.

O'Connell, B.C., and Harper, J.W. (2007). Ubiquitin proteasome system (UPS): what can chromatin do for you? Curr. Opin. Cell Biol. *19*, 206–214.

Puram, S.V., Kim, A.H., Ikeuchi, Y., Wilson-Grady, J.T., Merdes, A., Gygi, S.P., and Bonni, A. (2011a). A CaMKIIβ signaling pathway at the centrosome regulates dendrite patterning in the brain. Nat. Neurosci. *14*, 973–983.

Puram, S.V., Riccio, A., Koirala, S., Ikeuchi, Y., Kim, A.H., Corfas, G., and Bonni, A. (2011b). A TRPC5-regulated calcium signaling pathway controls dendrite patterning in the mammalian brain. Genes Dev. *25*, 2659–2673.

Riedinger, C., Boehringer, J., Trempe, J.F., Lowe, E.D., Brown, N.R., Gehring, K., Noble, M.E., Gordon, C., and Endicott, J.A. (2010). Structure of Rpn10 and its interactions with polyubiquitin chains and the proteasome subunit Rpn12. J. Biol. Chem. *285*, 33992–34003.

Rosenzweig, R., Bronner, V., Zhang, D., Fushman, D., and Glickman, M.H. (2012). Rpn1 and Rpn2 coordinate ubiquitin processing factors at proteasome. J. Biol. Chem. *287*, 14659–14671.

Stauffer, T.P., Ahn, S., and Meyer, T. (1998). Receptor-induced transient reduction in plasma membrane PtdIns(4,5)P2 concentration monitored in living cells. Curr. Biol. *8*, 343–346.

Takeuchi, J., Fujimuro, M., Yokosawa, H., Tanaka, K., and Toh-e, A. (1999). Rpn9 is required for efficient assembly of the yeast 26S proteasome. Mol. Cell. Biol. *19*, 6575–6584.

van Nocker, S., Sadis, S., Rubin, D.M., Glickman, M., Fu, H., Coux, O., Wefes, I., Finley, D., and Vierstra, R.D. (1996). The multiubiquitin-chain-binding protein Mcb1 is a component of the 26S proteasome in Saccharomyces cerevisiae and plays a nonessential, substrate-specific role in protein turnover. Mol. Cell. Biol. *16*, 6020–6028.

Varshavsky, A. (1996). The N-end rule: functions, mysteries, uses. Proc. Natl. Acad. Sci. USA *93*, 12142–12149.

Verma, R., Oania, R., Graumann, J., and Deshaies, R.J. (2004). Multiubiquitin chain receptors define a layer of substrate selectivity in the ubiquitin-proteasome system. Cell *118*, 99–110.

Yamada, T., Yang, Y., and Bonni, A. (2013). Spatial organization of ubiquitin ligase pathways orchestrates neuronal connectivity. Trends Neurosci. *36*, 218–226.

Young, P., Deveraux, Q., Beal, R.E., Pickart, C.M., and Rechsteiner, M. (1998). Characterization of two polyubiquitin binding sites in the 26 S protease subunit 5a. J. Biol. Chem. *273*, 5461–5467.